JOURNAL OF MECHANICAL ENGINEERING AND SCIENCES
ISSN: 2289-4659 e-ISSN: 2231-8380
VOLUME 18, ISSUE 2, 2024, 10004 – 10016
DOI: https://doi.org/10.15282/jmes.18.2.2024.3.0790

RESEARCH ARTICLE

Empowering industrial automation labs with IoT: A case study on real-time monitoring and control of induction motors using Siemens PLC and Node-RED

A. H. Embong, L. Asbollah, S. B. Abdul Hamid*

Department of Mechatronics Engineering, International Islamic University Malaysia, 53100 Kuala Lumpur, Wilayah Persekutuan, Malaysia
Phone: +6036423496

ABSTRACT - This initiative discusses the utilization of the Internet of Things (IoT) to enable smart control and monitoring of multiple devices in an industrial automation lab. The traditional manual approach of overseeing device performance in the industrial sector is prone to errors and lacks scalability and efficiency. The investigation compares Node-RED and Labview and proposes a design for remote control and monitoring. The process involves Node-RED, Siemens S7-1200 PLC, Sinamics V20 and an induction motor. Key steps include configuring frequency data exchange between Node-RED and the PLC, allocating frequencies based on an ID communication protocol, and using PLC data to power the induction motor via the Variable Frequency Drive. An experimental setup aims to validate the system's applicability and functionality by comparing theoretical data with experimental results. The study included a no-load test to observe motor shaft operation and a variable load setup where the motor was subjected to varying loads. Real-time monitoring of speed and torque adjustments was facilitated by the control unit. The no-load test revealed an average slip of 0.06 for the motor, with a direct voltage-frequency relationship. In the variable load test, the motor maintained a consistent voltage-to-frequency ratio, while current behaviour varied across different load ranges. By leveraging IoT connectivity using Siemens PLC S7-1200, this project demonstrates real-time data collection and analysis using Node-RED, Google Firebase, Google Sheets, and remote-control capabilities, leading to improved operational efficiency, reduced downtime, and increased productivity. The article emphasizes the significance of IoT in industrial automation labs and highlights its potential to revolutionize device control and monitoring, particularly focusing on the analysis of induction motors. The main challenge was to interface the devices to create an interconnected robust system, which was successfully overcome by implementing various IoT protocols. The system generated promising results, confirming IoT's potential in industrial automation.

ARTICLE HISTORY

Received	:	04th Aug. 2023
Revised	:	05th Apr. 2024
Accepted	:	27th May 2024
Published	:	28th June 2024

KEYWORDS
Node-RED
Induction motor
Internet of things
Variable frequency drive

1. INTRODUCTION

Control and monitoring of machines and devices in industrial application is desirable to assist user to perform maintenance before any failure occurs which subsequently avoids downtime [1, 2]. One of the main machines used predominantly in the industry is the induction motor due to its distinctive characteristics of the induction motor, such as its sturdy construction, cost-effective maintenance, high starting torque, efficiency, and reliability, set it apart from other types of motors [3]. In the past, manual control and monitoring of induction motors involved regular inspections, periodic maintenance schedules, and manual adjustments to ensure optimal performance [4]. Operators had to physically assess the motor's condition, measure parameters such as temperature, vibration, and current, and manually adjust voltage, frequency, or other control parameters as needed [5]. With the emergence of IoT in the control and monitoring of induction motors, the extraction of various important parameters of the motor in real time across distance has been become possible and easier to support different industries such as agriculture [6], smart city [7] and healthcare [8]. However, there are many ways that the IoT could be deployed using technique which includes use of PZEM-004T sensors [9], Blynk IoT application [9, 10] self-powered IoT nodes [10], ESP32 Module [11] and Raspberry-Pie [12]. This make the implementation of IoT within an industry to be challenging and each industry need to apply suitable framework to implement IoT based on required insight and the available sensors, actuators, and control availability.

One of the common speed controls of the motor is the utilizing the variable frequency drive (VFD) [13]. The most common method to control the speed of a motor is by utilizing voltage-to-frequency control method. This method involves varying the frequency and voltage proportionally while maintaining a consistent voltage-to-frequency ratio [14]. The integration of IOT technologies and VFD has enabled the mechanism of speed control remotely without the need for manual inspections and adjustments which subsequently can reduce downtime and real-time data collection. In the realm of remote motor operation control, Message Queue Telemetry Transport (MQTT) [15-17] emerges as a prominent platform. By integrating MQTT with a Variable Speed Drive (VSD), it becomes possible to regulate the speed of an

*CORRESPONDING AUTHOR | S. B. Abdul Hamid | ✉ syamsul_bahrin@iium.edu.my

induction motor by transmitting analog output data through an MQTT broker. This data is received by the VSD, which then adjusts the motor speed accordingly[18]. Furthermore, the implementation of sensors allows for the acquisition of real- time motor parameters, which can be transmitted via MQTT to the client for monitoring and analysis purposes.

Microcontrollers can also be utilized for remote control and monitoring [19, 20]. The integration of an ESP8266 Node MCU Devkit with a VFD for precise speed control of a three-phase induction motor is achievable by adjusting the motor's rotation speed through Wi-Fi connectivity and a dedicated mobile app, using a square wave generated by the Node MCU, the VFD alters the output currents [21]. The experimental setup featured a 0.5 HP induction motor driven by a Rhymebus Corporation VFD inverter, with a fixed operating frequency of 60 Hz. The remote control and monitoring of motor speed can be achieved through the utilization of Programmable Logic Controllers (PLCs). Previous research displays the OMRON CJ1M CPU11-ETN21 PLC integrated with LabVIEW and the NI OPC Server was employed for remote speed control [22]. User input was converted to Boolean data and transmitted via Ethernet, activating the relevant PLC outputs to control the OMRON SYSDRIVE 3G3MV-A2007 VFD. A virtual speed knob on the LabVIEW control panel facilitated the adjustment of motor speed by modifying the frequency of the VFD. Overall, this paper demonstrates the integration of IoT in an industrial automation lab, enabling smart control and monitoring of multiple devices. Through real-time data collection, analysis, and remote-control capabilities, it plans to enhance operational efficiency, reduce downtime, and increase productivity. The focus is on the potential of IoT to revolutionize device control, particularly in induction motor.

2. MATERIALS AND METHODS

2.1 Proposed Design

The proposed design for remote motor control and monitoring utilizing Node-RED [23] as shown in Figure 1 involves several key steps. Firstly, motor parameters are collected and sent to Firebase [24], a cloud-based database. From there, the data is extracted and transferred to Google Sheets for further analysis. Node-RED is employed as the central platform, connecting various components of the system. To enable an efficient system, two key elements within the framework are considered: (a) data transfer and connectivity, (b) real-time computation and data readability and (c) communication and data exchange capability.

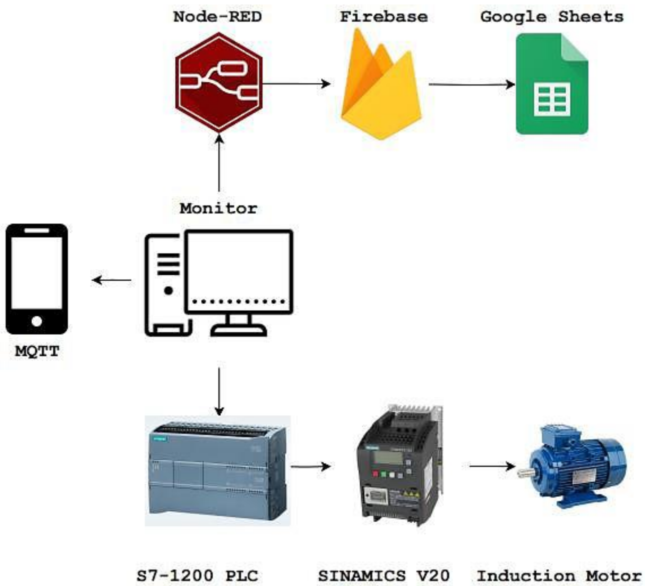

Figure 1. Proposed design for remote control and monitoring

2.2 Data Transfer and Connectivity

The system is integrated with MQTT for efficient data transfer and can be controlled through the IoT MQTT panel app. Simultaneously, Node-RED is connected to a Siemens PLC, which interfaces with the VFD and the induction motor. This comprehensive setup enables remote control and monitoring of the motor, with seamless communication between the different elements of the system. Based on previous research projects, LabVIEW has been predominantly utilized for control and data extraction [25-28]. However, considering the focus on IoT components, Node-RED has been chosen as the preferred software due to its extensive capabilities in connectivity. Table 1 shows the benefits of Node-RED compared to LabVIEW.

Table 1. Comparison between Node-Red and LabView

Functionality	Node-Red	LabView
Open Source	Yes	No
Web-based interface	Yes	No (Desktop application)
Rapid prototyping and development	Intuitive drag and drop interface	Visual, but steeper learning curve and setup time
Lightweight and scalable	Run and built on node.js	Powerful, but have limitations with scalability

2.2.1 Real-time computational and data readability

For real-time data computing of motor parameters, Google Firebase is selected as the platform due to its self-scaling and robust user-based security [29] to transfer data from Node-RED to Google Sheets. Google Firebase's real-time database [29] ensures immediate synchronization of data changes, allowing for prompt updates and inspections. In contrast, LabVIEW lacks native support for cloud-based storage and real-time synchronization, requiring additional components and manual integration with external databases, which makes this framework a much better IoT deployment. To enhance data readability, Google Sheets is integrated with Firebase, enabling the automatic transfer and update of motor parameter data. Google Apps Script is utilized to automate tasks within Google Sheets, allowing for the structured display and analysis of motor parameter data.

The Node-RED platform is utilized in this research have three main functions: (a) displaying real-time motor parameter data obtained from the S7-1200 PLC on a dashboard, (b) controlling motor speed by adjusting the frequency through a gauge display, and (c) storing motor parameter data in a real-time Firebase database. To enable communication with the S7-1200 PLC and Firebase, the necessary Node-RED packages for Siemens S7 Protocol and Firebase Realtime Database API must be installed. The Node-RED dashboard features a frequency gauge with a slider for frequency adjustment, a gauge and text display for motor speed, a graph illustrating current and voltage over time, and an option to select the motor's rotation direction. The GUI design of the dashboard is depicted in Figure 2, which showcases three distinct category blocks: motor settings, motor parameters and insight measurements of the motor.

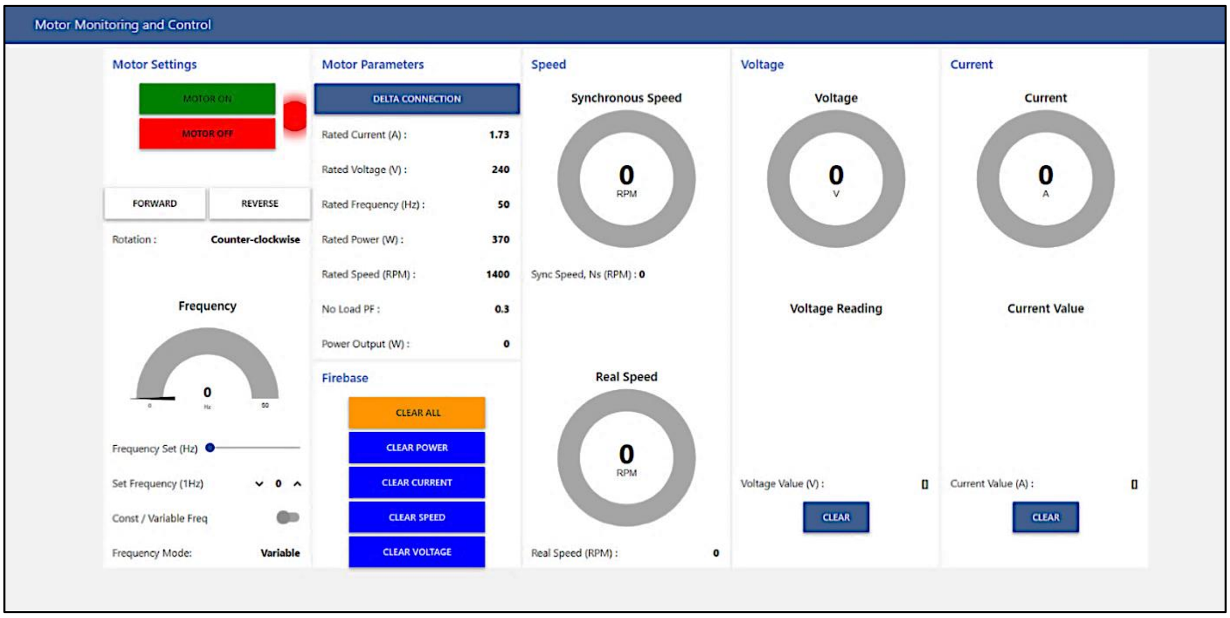

Figure 2. The Node-RED dashboard

The data transfer from Node-RED to Firebase is facilitated through the Firebase Realtime Database API, which is a cloud- hosted database that ensures real-time synchronization of data. The "firebase write" node is employed to transmit voltage, current, and speed input data obtained from the PLC's "s7 in" node to the designated paths in the Firebase Realtime Database. Correct configuration of the nodes with the Firebase project's credentials and accurate specification of the paths are necessary for proper data storage and retrieval. In this project, the voltage, current, and speed of the motor are designated as the main paths, while additional parameters such as motor frequency, motor status, and power are included to enhance monitoring capabilities. Figure 3 illustrates the setup of the real-time database in Firebase that could be configured by user.

Figure 3. Real-time database Firebase

2.2.2 Communication and data exchange capability

To enhance communication and data exchange capabilities of the system, the MQTT protocol is incorporated, enabling efficient connectivity between various devices. Specifically, the IOT MQTT panel app on a mobile phone is utilized, allowing bidirectional communication with Node-RED. The mobile phone acts as both a subscriber and publisher, enabling control over motor frequency and real-time monitoring of motor parameters through the app, like the Node-RED dashboard. This integration adds more functionality to the current system, facilitating seamless interaction between the user and the connected devices both from Node-RED and mobile app. Figure 4 portrays one of the insight a user could observed through the dashboard for mobile app using MQTT in two motor conditions: motor is running and motor in halt position.

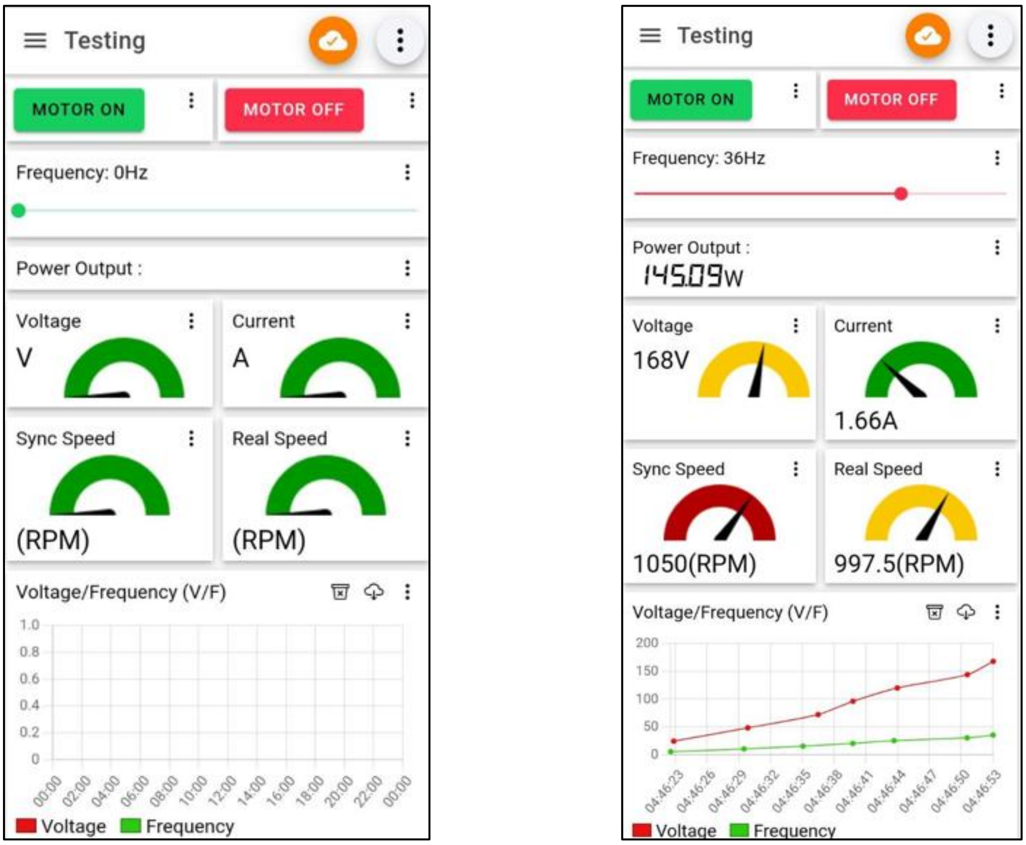

Figure 4. Real-time database Firebase

Lastly, the extracted data from Firebase is transferred to Google Sheets using Google Apps Script. By organizing the motor parameter data in a structured format within the spreadsheet, the data can be visualized through graphs and charts, enabling the verification of v/f, voltage, and current characteristics against motor specifications. Google Sheets storage is updated with new data every minute, automated through trigger feature in Google Apps Script, ensuring real- time data updates without manual intervention. This allows for continuous monitoring and comparison of theoretical and actual data from the VFD, providing valuable insights into the motor's performance. The display setup for Google Sheet database can be seen in Figure 5, which enables user to have insight of the motor condition.

Timestamp	Index	Motor Status	Frequency	Voltage	Current	Speed	Power
6/11/2023, 14:53:34	1	ON	1	4.8	7.12	28.5	17.76
6/11/2023, 14:53:34	2	ON	4	19.2	2.91	114	29
6/11/2023, 14:53:34	3	ON	7	33.6	2.3	199.5	40.23
6/11/2023, 14:53:34	4	ON	13	62.4	1.93	370.5	62.7
6/11/2023, 14:53:34	5	ON	14	67.2	1.9	399	66.44
6/11/2023, 14:53:34	6	ON	20	96	1.78	570	88.91
6/11/2023, 14:53:34	7	ON	28	134.4	1.7	798	118.88
6/11/2023, 14:53:34	8	ON	32	153.6	1.68	912	133.85
6/11/2023, 14:53:34	9	ON	34	163.2	1.67	969	141.34
6/11/2023, 14:53:34	10	ON	37	177.6	1.65	1054.5	152.58
6/11/2023, 14:53:34	11	ON	38	182.4	1.65	1083	156.32
6/11/2023, 14:53:34	12	ON	41	196.8	1.64	1168.5	167.56
6/11/2023, 14:53:34	13	ON	36	172.8	1.66	1026	148.83
6/11/2023, 14:53:34	14	ON	33	158.4	1.67	940.5	137.6
6/11/2023, 14:53:34	15	ON	32	153.6	1.68	912	133.85
6/11/2023, 14:53:34	16	ON	28	134.4	1.7	798	118.88
6/11/2023, 14:53:34	17	ON	25	120	1.73	712.5	107.64
6/11/2023, 14:53:34	18	ON	33	158.4	1.67	940.5	137.6
6/11/2023, 14:53:34	19	ON	40	192	1.64	1140	163.81
6/11/2023, 14:53:34	20	ON	41	196.8	1.64	1168.5	167.56
6/11/2023, 14:53:34	21	ON	43	206.4	1.63	1225.5	175.05
6/11/2023, 14:53:34	22	ON	46	220.8	1.62	1311	186.28

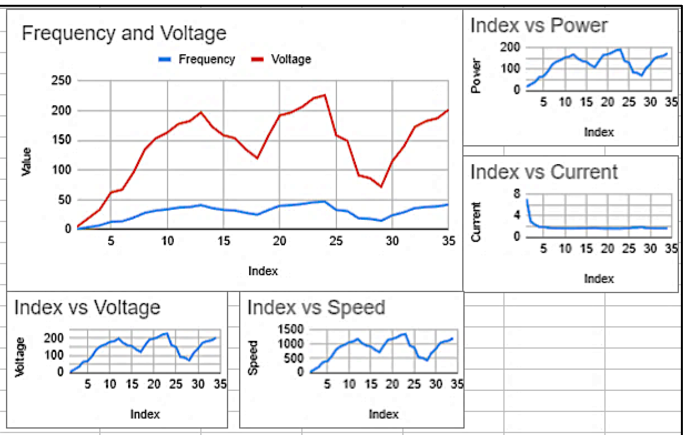

Figure 5. Google sheet database

2.3 Proposed Motor Parameter, Control and Data Flow

2.3.1 Motor parameter acquisition and data flow pipeline

Data acquisition is the process of gathering and measuring data from various sources, including numerical data from computers and physical measurements from sensors. In this research, the focus is on motor parameters such as current, voltage, and speed. These parameters can be extracted from the SINAMICS V20 drive to the S7-1200 PLC using two methods: Universal Serial Interface (USS) and Modbus. USS allows standardized communication between the master device and specific VFDs, enabling control and monitoring of parameters. Modbus, on the other hand, is a widely used protocol that facilitates communication with various industrial equipment, including VFDs. However, due to limitations in the available analog signal board, data extraction directly from the VFD is not possible. Therefore, theoretical calculations will be used for data analysis and comparison with experimental values.

By utilizing theoretical data calculations, a data flow pipeline is established among Node-RED, MQTT IoT Panel app, Firebase, and Google Sheets. Node-RED facilitates real-time data exchange with the MQTT IoT Panel app, followed by data transfer to Firebase for storage using the Firebase Realtime Database API. Subsequently, the extracted data is seamlessly transmitted to Google Sheets through Google Apps Script for effective visualization and analysis. The flow of data can be seen in Figure 6. The motor parameters to be monitored in this research are the input voltage, stator current, and motor speed. These parameters are closely tied to the motor specifications, and it is crucial to consider these specifications when determining the theoretical values for each parameter. Two induction motors are used in the experiment, one connected to the IOT kit and another available in the Electromechanical lab. The specifications of the motors are provided along with a corresponding image. Table 2 presents the parameter of the induction motor used for no-load experiment and variable load experiment.

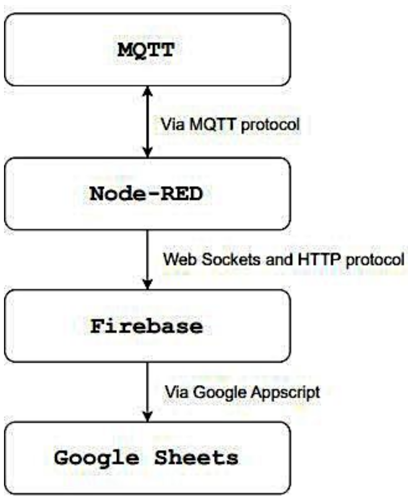

Figure 6. Data flow pipeline

Table 2. Parameter of induction motor for no-load experiment and variable load experiment

Motor Parameter	no-load experiment	variable load experiment
Poles	4	4
Rated Frequency	50 Hz	50
Rated Speed	1400 RPM	1500
Rated Power	0.37k W	0.27 kW
Rated Voltage (Delta Connection)	220-240 V	230 V
Rated Current (Delta Connection)	1.88-1.73 A	1.44 A

2.3.2 Motor control mechanism: Varying frequency for speed control

The data transmission between software and hardware components involves communication protocols. The speed control of the induction motor is achieved by adjusting the VFD frequency using the voltage/frequency method. This method maintains a constant voltage-to-frequency ratio while varying the frequency of the applied voltage to the motor. Figure 7 portrays the flow of the mechanism of motor control from Node-Red to Induction Motor.

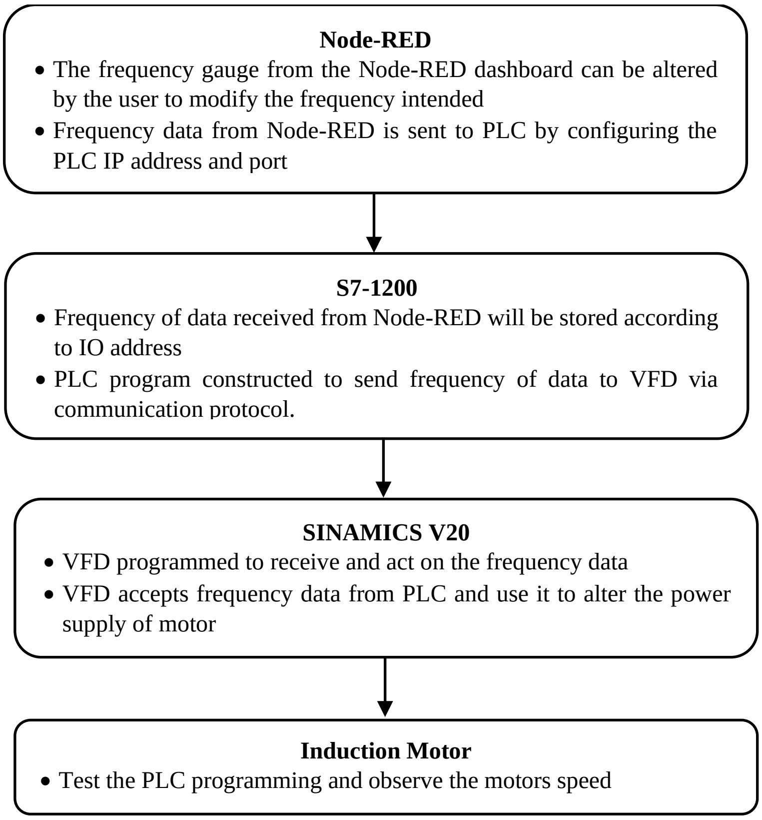

Figure 7. Flow of mechanism of motor control

The speed control of the induction motor is achieved by varying the frequency from the VFD, utilizing the voltage/frequency (*v*/*f*) control method. This widely employed method in industrial applications adjusts the frequency of the applied voltage to the motor while maintaining a constant voltage-to-frequency ratio. The manipulation of the VFD's supply frequency is accomplished through an analog output voltage module integrated into the PLC. This module interfaces with the PLC to generate an analog output voltage within the 0- 10 V range, thereby influencing the motor's frequency. The VFD's internal control mechanism interprets the analog voltage signal and converts it into the appropriate frequency output.

2.4 Theoretical Modelling

The control method used for the induction motor from the VFD is the v/f method. This method ensures that the voltage supplied to the motor increases proportionally with the frequency. This is done to maintain a constant voltage-to-frequency ratio, which is vital for the motor's optimal performance and consistent magnetic field strength at different frequencies. The formula to formulate the voltage to the motor with respect to frequency supplied can be seen in Eq. (1).

$$V = kf \tag{1}$$

where, k is the voltage to frequency ratio, which is the ratio of the nominal voltage, V to the nominal frequency, f of the motor.

Hence, the k constant was obtained for the induction motor used for no load test to be 4.6 and 4.8 for induction motor used for variable load test for rated voltage of 230V-240V and rated frequency of 50 Hz respectively. Next, the synchronous speed of an induction motor can be determined by Eq. (2), where it is the ratio of the multiplied frequency with 120 over the number of poles of the motor, p. From the synchronous speed, the rotor speed is calculated as n_r using the slip, s in Eq. (3), which accounts for the difference between the synchronous speed and the actual speed of the motor.

$$n_s = \frac{120f}{p} \tag{2}$$

$$n_r = sn_s \tag{3}$$

Genuinely, the slip for the motor will be low for no load experiment due to the minimal mechanical resistance or load on the motor shaft. As a result, the rotor speed will be close to the synchronous speed, and the slip value will approach zero. This is a contrast with the variable load experiment, where the presence of mechanical resistance or load on the motor shaft causes an increase in slip. As the load on the motor increases, the slip value will also increase, resulting in a deviation from the synchronous speed and a lower rotor speed compared to the no-load condition. The current drawn by the motor under load conditions will show contrasting results compared to the no-load condition, with the motor's speed exhibiting a significant decrease and the current drawn increasing to provide necessary torque. The voltage will still proportionally increase with frequency due to the *v/f* control method, while the current is expected to decrease at higher frequencies due to reduced magnetizing current, core losses, and windage/friction loss.

2.5 Experimental Setup

The experiment setup is used to verify whether the system constructed is applicable and functioning whilst comparing theoretical data and experimental data. The experimental test setup for no-load is shown in Figure 8 which has 3 main components namely computer for insight display (left), IoT kit (center), induction motor (right).

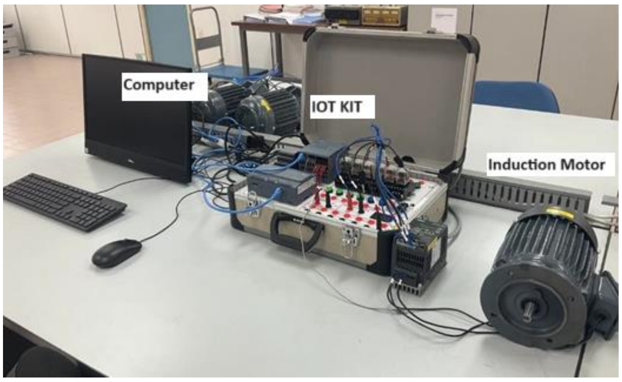

Figure 8. No-load experimental setup

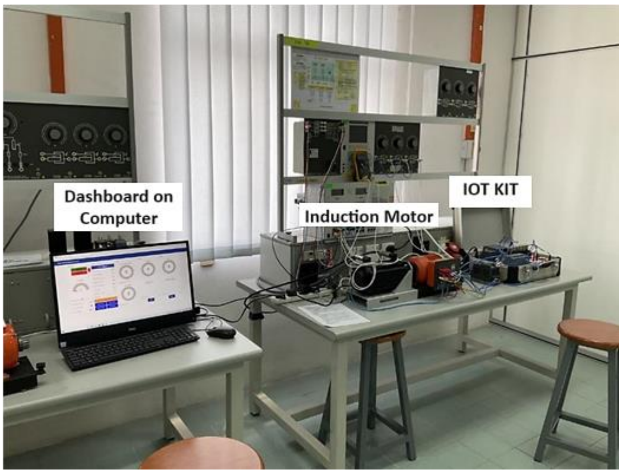

Figure 9. Experiment setup for variable load

The no-load test is performed in the control system laboratory to observe the motor's shaft operation without any load. On the other hand, the variable load setup is conducted in the Electromechanical laboratory using available lab equipment to apply different loads. Figure 9 illustrates the experimental setup for the variable load test. In the research study, the variable load experimental setup was employed to investigate the motor's performance. This setup involved a servo motor that applied a variable load to the motor by rotating in the opposite direction. The control unit allowed for real-time observation of the motor's actual speed while adjusting the torque applied to the motor. The components utilized in the variable load setup can be seen in Figure 10.

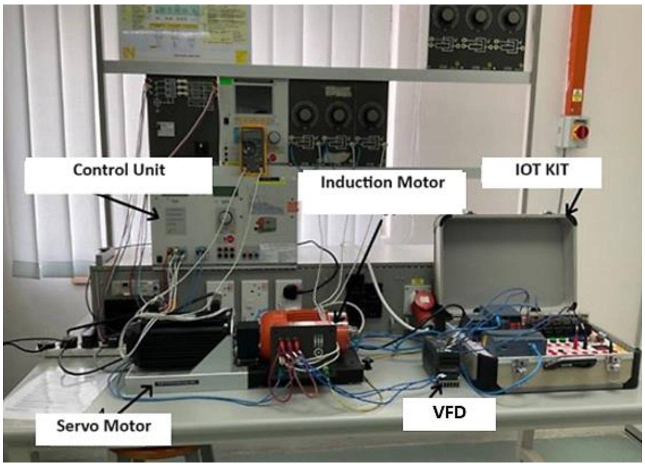

Figure 10. Components utilized in the variable load setup

3. RESULTS AND DISCUSSION

3.1 No Load Test

To analyze the slip of the induction motor under no-load conditions, the motor's shaft is subjected to testing using a tachometer. During no load, the rotational speed of the rotor closely aligns with the rotating magnetic field, resulting in a low slip. The corresponding motor speed readings are presented in Table 3.

Table 3. Real speed and synchronous speed of motor at different frequencies at no-load

Frequency (Hz)	Synchronous speed (RPM)	Actual speed (RPM)
10.34	310.2	307.7
20.30	609.0	606.6
30.32	909.6	906.7
40.32	1209.6	1201.0
50.00	1500.0	1486.0

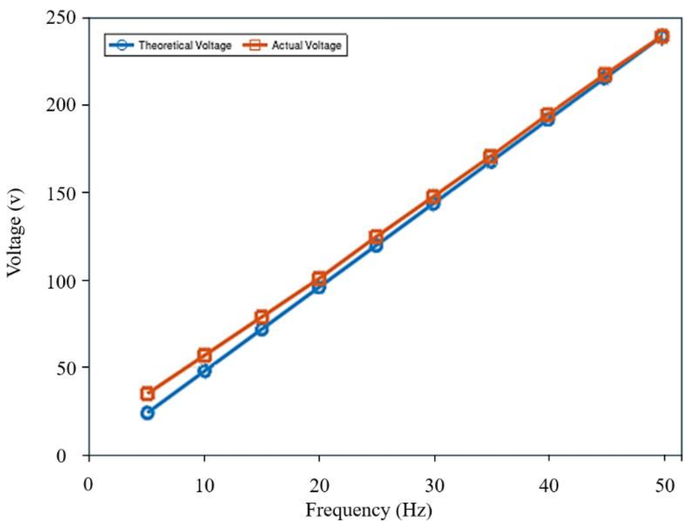

Figure 11. Plot of the calculated voltage and actual voltage using v/f method

The average slip, $\overline{X_{slip}}$ for the induction motor is determined by calculating the average value of slip across five distinct frequencies using the Eq. (4) as observed from the data presented in Table 3. The slip obtained for the motor at no-load is 0.06. Next, the test is conducted by increasing the frequency by 5 Hz each interval until the maximum frequency is obtained. The readings for the voltage and frequency are shown in Figure 11. From the plot, the analysis of VFD readings reveals a direct relationship between voltage and frequency, indicating a linear correlation. However, it is important to note that the experimental voltage readings slightly deviate from the theoretically calculated values due to the assumption of steady state conditions in the calculations, which may not account for non-linearities introduced by the motor and its associated components. The results are also observed by Xu et al. [30] where it is it was found that voltage sags significantly impact the performance of low-voltage VFD, necessitating consideration of non-linearities introduced by motors and associated components.

$$\overline{X_{slip}} = \sum \left[\left(\frac{(N_s - N)}{N_s} \right) /5 \right] \tag{4}$$

where, N and N_s are the rotor speed/real speed and synchronous speed, respectively.

The graph of current over frequency, as shown in Figure 12, exhibits a high current value at low frequencies that gradually decreases and stabilizes at the maximum frequency. This behavior can be attributed to the *v/f* control technique, where the applied voltage is significantly lower at low frequencies compared to the rated voltage. Consequently, it takes longer for the magnetic flux to reach its maximum value, allowing the motor's magnetic core to approach or even reach saturation. When the core saturates, the relationship between magnetic flux and applied voltage becomes non-linear, resulting in increased magnetic reluctance within the motor. This increased reluctance necessitates a higher amount of magnetic flux to maintain the same magnetic field strength, thereby requiring a larger current. Consequently, the no-load current increases as the motor compensates for the reduced magnetic field at low frequencies by drawing more current. The impact of magnetic saturation in permanent magnet synchronous motors used for applications requiring constant power operation has also been highlighted by Marimoto et al. [31] where it was found that the motor parameters vary due to magnetic saturation, affecting control performance.

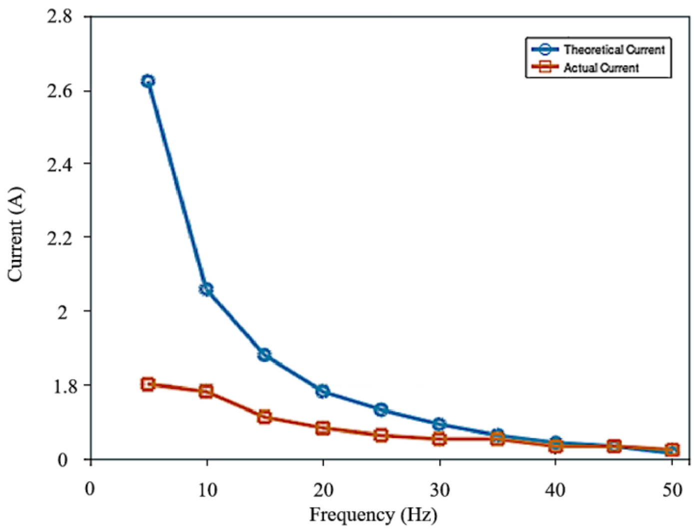

Figure 12. Comparison plot of the actual current reading and theoretical reading

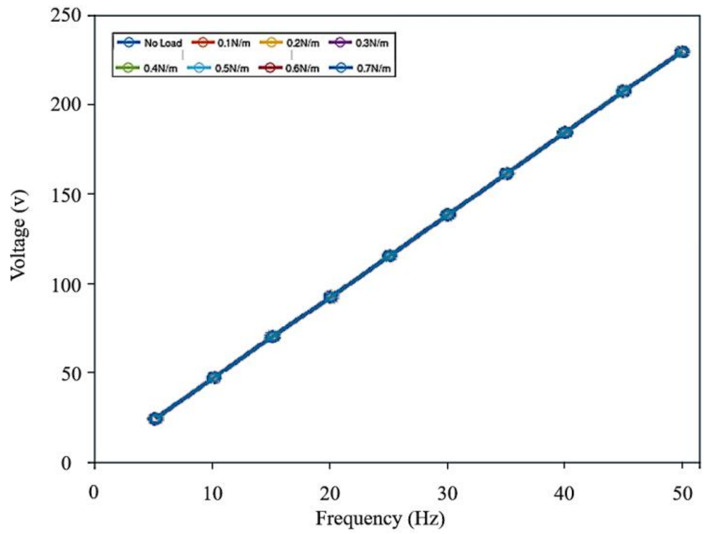

Figure 13. Voltage and frequency under variable load conditions

3.2 Variable Load Test

The variable load test aims to investigate the impact of different loads on motor parameters and observe their behavior. In the case of the voltage-to-frequency (*v*/*f*) control method, which is typically implemented as an open-loop system without feedback, the test aims to maintain a constant voltage-to- frequency ratio while subjecting the motor to varying loads. As the *v*/*f* control technique does not actively adjust motor parameters based on feedback, the test results provide insights into the motor's performance under changing load conditions while the control system maintains a consistent *v*/*f* ratio. As observed in the previous no-load experiment, the voltage- to-frequency ratio in the control of the motor remains consistent even when subjected to variable loads. This means that the ratio of voltage to frequency is maintained at a constant level regardless of the changes in the applied load. This can be observed from Figure 13. The graph depicted in Figure 14 illustrates the real speed of the motor under variable load conditions. The trend observed across different loads shows that as the frequency increases, the motor speed also increases. However, it is noteworthy that with each increase in load, the initial speed of the motor decreases, even at similar frequencies. This behavior can be attributed to the concepts of rotor speed and slip. During the previous no- load test, the motor's actual speed closely matched the synchronous speed, indicating a small slip value. Conversely, when a load is applied, the mechanical resistance acts against the rotor's rotational motion, causing a decrease in rotor speed and subsequently an increase in slip value.

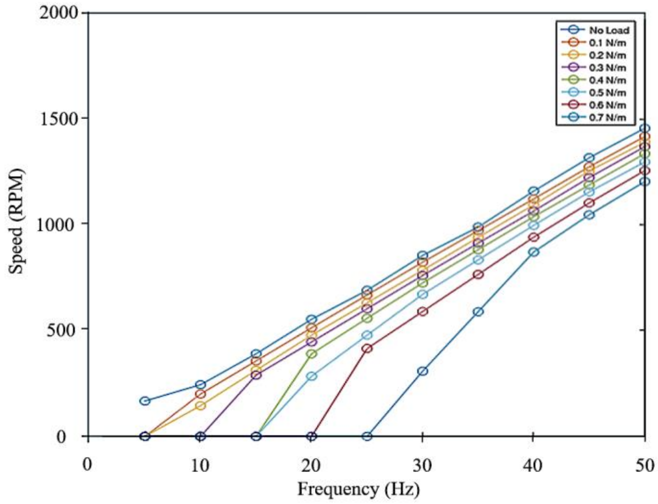

Figure 14. Speed of induction motor at different load

The current behavior of the motor under variable load conditions is depicted in Figure 15. As the v/f control is an open- loop system, the current does not increase with frequency since there is no feedback mechanism. Instead, the system maintains the voltage-to-frequency ratio. Examining the graph, it is evident that the motor current increases as the variable load is applied. In the low-load range of 0.1 N/m to 0.3 N/m, the current gradually rises with increasing frequency. This rise in current allows the motor to generate the required torque to overcome the load resistance, compensating for the additional mechanical load and maintaining the desired speed.

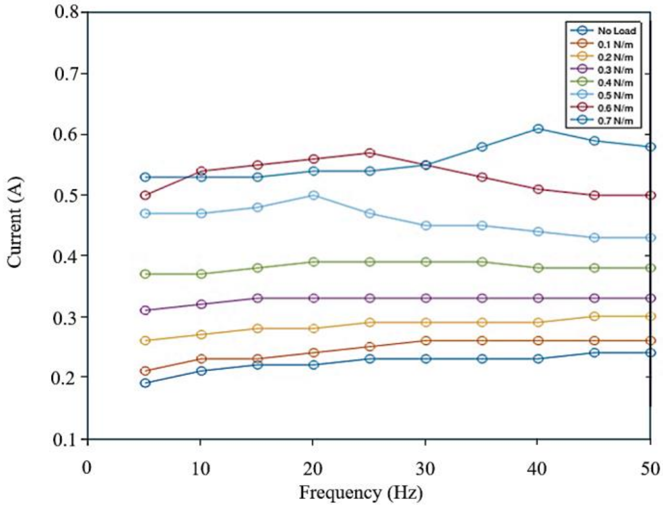

Figure 15. Current reading when applied with variable load

For higher loads ranging from 0.4 N/m to 0.7 N/m, a similar trend is observed, where the current initially increases with low frequencies. However, at high frequencies, the current starts to decrease. This can be attributed to two main factors. Firstly, the motor's impedance becomes more influential as the frequency increases, resulting in increased reactance and reduced current flow through the windings. Secondly, core losses, including hysteresis and eddy current losses, become more significant at higher frequencies, leading to increased power dissipation, and reduced effective current in the windings. The experimental results obtained from both the no-load and variable load tests provide valuable insights into the behavior of the induction motor. Under the no-load condition, the motor's speed closely matched the synchronous speed with minimal slip, demonstrating the effectiveness of the voltage-to- frequency (v/f) control method in maintaining a constant voltage-to-frequency ratio. However, when subjected to variable loads, the motor exhibited changes in speed at similar frequencies, indicating the influence of mechanical resistance and increased slip. Furthermore, the current drawn by the motor showed a direct relationship with the applied load, allowing the motor to generate the necessary torque. At higher loads, the current initially increased with low frequencies but decreased at high frequencies, influenced by factors such as motor impedance and core losses. These findings contribute to our understanding of motor performance under different load conditions and highlight the importance of considering control strategies for optimal operation.

4. CONCLUSIONS

In summary, the project has successfully achieved integrating IoT protocols for effective communication between the Node-RED interface and the VFD. This integration enabled efficient control and monitoring of motor operation through an IoT system. Additionally, a cloud-based solution was developed to transmit motor parameters across different software platforms, facilitating real-time monitoring, parameter storage, and simplified data analysis with remote access capabilities. The integration of the Node-RED interface with the VFD improved motor control and monitoring, enhancing operating efficiency and flexibility. The system was successfully implemented and tested in the Industrial Automation Lab, demonstrating the motor's performance under variable load conditions while maintaining a constant *v/f* ratio. These could be shown through the different results such as the no-load test which revealed an average slip of 0.06 for the motor, with a direct voltage-frequency relationship and in in the variable load test where the motor maintained a consistent voltage-to-frequency ratio, while indicating a current behaviour which varied across different load ranges. The framework, implementation, and results from the IoT enabled system, indicate two aspects: possibility of performing remote laboratory within the context of education and the possibility of an engineer performing remote control, monitoring and when coupled with machine learning perform predictive maintenance for an induction motor.

ACKNOWLEDGMENTS

The authors would like to acknowledge International Islamic University Malaysia and IOT Sata Sdn. Bhd. for installation of the industrial automation system.

CONFLICT OF INTEREST

The authors declare that they do not have any conflict of interest.

AUTHORS CONTRIBUTION

A. H. Embong (Supervision; Experimental framework; Data analysis; Wring - original draft)
L. Asbollah (Experimental work; Data curation; Writing – original draft)
S. B. Abdul Hamid (Data analysis; Experimental work; Writing – review and editing)

REFERENCES

[1] R. Kothamasu, S. H. Huang, W. H. Verduin, "System health monitoring and prognostics - A review of current paradigms and practices," *International Journal of Advanced Manufacturing Technology*, vol. 28, no. 9, pp. 1012–1024, 2006.

[2] R. C. M. Yam, P. W. Tse, L. Li, P. Tu, "Intelligent predictive decision support system for condition-based maintenance," *International Journal of Advanced Manufacturing Technology*, vol. 17, no. 5, pp. 383–391, 2001.

[3] D. Shyamala, D. Swathi, J. L. Prasanna, A. Ajitha, "IoT platform for condition monitoring of industrial motors," in *Proceedings of the 2nd International Conference on Communication and Electronics Systems (ICCES2017)*, vol. 2018, pp. 260–265, 2018.

[4] A. K. S. Jardine, D. Lin, D. Banjevic, "A review on machinery diagnostics and prognostics implementing condition-based maintenance," *Mechanical Systems and Signal Processing*, vol. 20, no. 7, pp. 1483–1510, 2006.

[5] B. V. Divya, N. Latha, P. Ashwinikumari, "IOT enabled power monitoring and control of single-phase induction motor," in *International Conference on Emerging Smart Computing and Informatics (ESCI2021)*, pp. 670–673, 2021.

[6] J. C. Zhao, J. F. Zhang, Y. Feng, J. X. Guo, "The study and application of the IoT technology in agriculture," in *Proceedings of 3rd IEEE International Conference on Computer Science and Information Technology (ICCSIT2010)*, vol. 2, pp. 462–465, 2010.

[7] M. M. Rathore, A. Paul, W. H. Hong, H. C. Seo, I. Awan, S. Saeed, "Exploiting IoT and big data analytics: Defining smart digital city using real-time urban data," *Sustainable Cities and Society*, vol. 40, pp. 600–610, 2018.

[8] R. K. Kodali, G. Swamy, B. Lakshmi, "An implementation of IoT for healthcare," in *IEEE Recent Advances in Intelligent Computational Systems (RAICS2015)*, pp. 411–416, 2016.

[9] R. Syawali, S. Meliala, "IoT-based three-phase induction motor monitoring system," *Journal of Renewable Energy, Electrical, and Computer Engineering*, vol. 3, no. 1, pp. 12–18, 2023.

[10] A. Firmansah, N. Mufti, A. N. Affandi, I. A. E. Zaeni, "Self-powered IoT based vibration monitoring of induction motor for diagnostic and prediction failure," in *IOP Conference Series: Materials Science and Engineering*, p. 012016, 2019.

[11] A. Shukla, S. P. Shukla, S. T. Chacko, M. K. Mohiddin, K. A. Fante, "Monitoring of single-phase induction motor through IoT using ESP32 module," *Journal of Sensors*, vol. 2022, p. 8933442, 2022.

[12] N. Dehbashi, M. SeyyedHosseini, A. Yazdian-Varjani, "IoT based condition monitoring and control of induction motor using raspberry pi," in *IEEE 13th Power Electronics, Drive Systems, and Technologies Conference (PEDSTC2022)*, pp. 134–138, 2022.

[13] Y. Li, "Variable frequency drive applications in HVAC systems," *New Applications of Electric Drives*, pp. 167–185, 2015.

[14] B. J. Sauer, P. A. Brady, "Application of AC induction motors with variable frequency drives," in *IEEE Cement Industry Technical Conference*, pp. 1-10, 2009.

[15] B. Ganguly, A. Chatterjee, "MQTT protocol based extensive smart motor control for electric vehicular application," in *7th IEEE Uttar Pradesh Section International Conference on Electrical, Electronics and Computer Engineering (UPCON2020)*, pp. 1-5, 2020.

[16] A. Bhawiyuga, M. Data, A. Warda, "Architectural design of token-based authentication of MQTT protocol in constrained IoT device," in *Proceeding of 11th International Conference on Telecommunication Systems Services and Applications (TSSA2017)*, vol. 2018, pp. 1–4, 2018.

[17] M. Kazmi, M. T. Shoaib, A. Aziz, H. R. Khan, S. A. Qazi, "An efficient IoT-based smart sensor node for predictive maintenance of induction motors," *Computer Systems Science and Engineering*, vol. 47, no. 1, pp. 255-272, 2023.

[18] A. O. Kurniawan, A. R. Hakiki, K. N. Banjarnahor, M. A. Hady, A. Santoso, A. Fatoni, "Internet based remote laboratory architecture for 3-phase induction motor control system experiment," in *Proceedings of International Seminar on Intelligent Technology and Its Application: Intelligent Systems for the New Normal Era (ISITIA2021)*, pp. 381–385, 2021.

[19] M. M. Ali, S. H. Hussaini, M. Z. Uddin Abbas, M. Z. Ul Abedin, M. H. Khan, M. Omair, et al., "Microcontroller application in industrial control & monitoring systems," *International Journal of Engineering Trends and Technology*, vol. 17, pp. 26–31, 2014.

[20] I. Ahmed, H. Wong, V. Kapila, "Internet-based remote control using a microcontroller and an embedded ethernet," in *Proceedings of the American Control Conference*, vol. 2, pp. 1329–1334, 2004.

[21] G. -M. Sung, Y. -S. Shen, L. T. Keno, C. -P. Yu, "Internet-of-things based controller of a three-phase induction motor using a variable-frequency driver," in *IEEE Eurasia Conference on IOT, Communication and Engineering (ECICE2019)*, pp. 156-159, 2019.

[22] N. N. Barsoum, P. R. Chin, "Ethernet control AC motor via PLC using LabVIEW," *Journal of Intelligent Control and Automation*, vol. 2, no. 4, pp. 330–339, 2012.

[23] M. Tabaa, B. Chouri, S. Saadaoui, and K. Alami, "Industrial communication based on Modbus and Node-RED," *Procedia Computer Science*, vol. 130, pp. 583–588, 2018.

[24] L. Moroney. The Firebase Realtime Database: The Definitive Guide to Firebase, 1st ed. United States: Apress Berkely CA, pp. 51-71, 2017.

[25] P. Pillay, Z. Xu, "Labview implementation of speed detection for mains-fed motors using motor current signature analysis," *IEEE Power Engineering Review*, vol. 18, no. 6, pp. 47–48, 1998.

[26] S. Janrao, R. Ambekar, "Fault diagnosis of a braoken rotor bar in an induction motor using motor current signature analysis," *International Journal of Applied Engineering Research*, vol. 13, no. 12, pp. 11002 – 11008, 2018.

[27] J. Jerome, A. P. Aravind, V. Arunkumar, P. Balasubramanian, "LabVIEW based intelligent controllers for speed regulation of electric motor," *IEEE Instrumentation and Measurement Technology Conference*, vol. 2, pp. 935–940, 2005.

[28] P. Pillay, Z. Xu, "Motor current signature analysis," *IEEE Industry Applications Society Annual Meeting*, vol. 1, pp. 587–594, 1996.

[29] N. Nguyen, "Building an E-commerce application utilizing firebase cloud service," *Bachelor Thesis*, Metropolia University of Applied Sciences, Finland, 2022.

[30] Y. Xu, W. Lu, C. Li, W. Aslam, "Sensitivity of low-voltage variable-frequency devices to voltage sags," *IEEE Access*, vol. 7, pp. 2068–2079, 2019.

[31] S. Morimoto, M. Sanada, Y. Takeda, "Effects and compensation of magnetic saturation in flux-weakening controlled permanent magnet synchronous motor drives," *IEEE Industry Application Society Annual Meeting*, vol. 30, no. 6, p. 1632.

[32] T. H. Morgan, W. E. Brown, A. J. Schumer, "Induction-motor characteristics at high slip," Electrical engineering, vol. 59, no. 8, pp. 464–468, 1940.